

Energy Efficiency in Low Voltage Hall Thrusters

Jerry L. Ross *

Lyon B. King †

Energy efficiency measurements were taken on a 2 kW (nominal) Hall thruster operating at discharge voltages of 100-200 V and 3 mg/s of xenon. Acceleration and current efficiencies were compared to thrust efficiency over a range of magnet coil current values of 0 A - 2.5 A. Acceleration efficiencies were obtained with a 4-grid Retarding potential analyzer and current efficiency measurements were calculated from the discharge current as read from the power supply maintaining the anode-cathode potential. The acceleration efficiency and current efficiency were divergent in the region of maximum thrust efficiency. Acceleration efficiency increased with decreasing magnet current where the cathode-to-ground potential was determined to account for a portion of the increase in the region of interest.

Nomenclature

\dot{m}	flow rate of propellant as determined by the mass flow controller
ϵ_i	ion energy
η_a	acceleration efficiency
η_β	beam divergence as an efficiency
η_c	current efficiency
η_e	energy efficiency
η_p	propellant efficiency
η_T	thrust efficiency
Φ_{CTG}	cathode-to-ground potential (< 0)
Φ_{max}	maximum available acceleration potential
\mathbf{V}	ion velocity vector
e	elementary charge
f_i	ionization mass fraction
I_d	discharge current
I_{sp}	specific impulse
M	mass of a xenon atom/ion
P	power
P_s	$I_d V_d$
P_{in}	P_s
P_{out}	kinetic power in the beam
Q	average particle charge number
q	particle charge number
T	thrust

*PhD Candidate, Michigan Technological University, Houghton MI, student member

†Associate Professor, Michigan Technological University, Houghton MI, member

U_e	ion velocity
V_d	discharge voltage (anode potential)
V_{accel}	acceleration potential for a given ion
V_{eff}	effective acceleration potential
V_{plasma}	plasma-to-ground potential

I. Introduction

Within the field of electric propulsion there is a high demand for systems of increased thrust capabilities. In part, this is due to a growing interest in using electric propulsion devices for orbit raising applications.¹ Orbit raising missions inherently require more thrust than station keeping. The thrust to power ratio is equal to

$$\frac{T}{P_s} = \frac{2\eta_T}{U_e} \quad (1)$$

This ratio is of the utmost importance because spacecraft power supplies are limited in their throughput. Hence, to increase the thrust of an electric propulsion thruster, while maintaining a constant power, U_e must be decreased while maintaining η_T . The exit velocity, U_e , is related to discharge voltage by

$$\frac{1}{2}MU_e^2 = qeV_{accel} \quad (2)$$

where $V_{accel} \approx V_d$.

For Hall thrusters, it has been shown that decreasing discharge voltage much below 300 V results in poor performance (low efficiency).² This study is a part of a continuing effort to understand the efficiency loss mechanisms of Hall thrusters at low voltages.

In a preceding study of the efficiency of a BPT-2000 (nominally 2 kW) Hall thruster operating at low discharge voltages, various loss mechanisms were explored at the maximum obtainable thrust efficiency.³ The study was conducted as a function of discharge voltage where thrust efficiency was calculated from thrust stand data, discharge supply measurements, and propellant line flow rates. The operating point corresponding to maximum efficiency was found by adjusting the current through the magnet coils. The results of the study showed that at low discharge voltages the maximum thrust efficiency did not correspond to the minimum discharge current. This finding was in conflict with existing data at higher discharge voltages, where it is well known that thrust efficiency peaks when the discharge current is minimized by magnet tuning.⁴ Excess discharge current is a loss mechanism accounted for in the current efficiency. Since the current efficiency was off peak, it indicated one or more loss mechanisms were inversely proportionate to current efficiency in the vicinity of maximum thrust efficiency.

In the study of low discharge voltages,³ the acceleration efficiency was observed to increase in value at three of the lowest discharge voltages. These results suggest that the acceleration efficiency could be inversely related to the current efficiency and responsible for the discrepancy between maximum current efficiency and maximum thrust efficiency at low discharge voltages. The goals of this study were to (1) determine if the acceleration efficiency is divergent with respect to current efficiency and (2) establish the physical mechanism responsible for increased acceleration efficiency at low discharge voltages.

II. Efficiency Analysis

Hall thruster efficiency is a term that is varied in its use within the community. Thrust stand measurements are combined with discharge current and voltage measurements and mass flow rates

as determined by the flow controllers to calculate thrust efficiency

$$\eta_T = \frac{T^2}{2\dot{m}P_s}. \quad (3)$$

Energy efficiency is the measure of power supply output conversion to kinetic energy in the beam

$$\eta_e = \frac{P_{out}}{P_{in}}, \quad (4)$$

where

$$P_{in} = I_d V_d \quad (5)$$

and

$$P_{out} = \frac{1}{2}\dot{m}\langle \mathbf{V}^2 \rangle. \quad (6)$$

Thrust efficiency is the product of energy efficiency and propellant efficiency $\eta_T = \eta_p \eta_e$ where

$$\eta_p = \frac{\langle \mathbf{V} \rangle^2}{\langle \mathbf{V}^2 \rangle}, \quad (7)$$

and \mathbf{V} is the ion velocity vector .

The propellant efficiency includes efficiencies regarding the collimation of the beam and the ionization efficiency that are not part of this study. A more rigorous distinction between energy and thrust efficiencies is outlined in Larson's work.⁴

Energy efficiency can be further broken down as the product of acceleration efficiency and current efficiency. Acceleration efficiency is

$$\eta_a = \frac{\frac{1}{2}M \langle \mathbf{V}^2 \rangle}{eV_d} \frac{1}{f_i Q} \quad (8)$$

and current efficiency is

$$\eta_c = \frac{\dot{m}e}{MI_d} (f_i Q) \quad (9)$$

where Q equals

$$Q = \frac{1}{f_i} (f_1 + 2f_2 + 3f_3).$$

The variable f_i is the ionization mass fraction of the propellant

$$f_i = f_1 + f_2 + f_3..$$

$$f_0 + f_i = 1$$

where f_0, f_1, f_2, f_3 are the exit mass fractions of $Xe, Xe^+, Xe^{++}, Xe^{+++}$.

III. Equipment

All measurements were taken on an Aerojet BPT-2000 Hall thruster designed to operate nominally between 300 V and 500 V.⁵ The xenon testing facility is a 2-m diameter and 4-m long vacuum chamber. Rough vacuum is reached by a 400-cfm two-stage rotary oil-sealed pump. High vacuum is reached and maintained by two 48-inch cryopumps that operate at 120,000 L/s (N_2). Chamber base pressure was $1 \cdot 10^{-6}$ Torr and the pressure did not exceed $4 \cdot 10^{-5}$ Torr during operation. Thrust measurements were taken by the use of a NASA Glenn inverted-pendulum thrust stand.⁶ The thrust stand is water cooled to alleviate thermal drifts and its level is monitored by a tilt sensor

accurate to one half an arc second. Anode and cathode propellant lines are controlled by MKS Type 1479A Mass-Flo[®] controllers. The propellant flow rate for all trials was 3 mg/s of xenon. A laboratory-grade LaB₆ cathode was used for testing (excerpt from reference³).

Acceleration efficiencies were obtained by a 4-grid RPA probe placed 500 mm downstream from the thruster faceplate on the thruster centerline. The RPA probe uses a series of biased grids to repel ions of low energy. Sweeping the retarding potential on the grids yields an ion energy-per-charge distribution function of the plume of the Hall thruster. The RPA grid wires are .0045" in diameter with .0055" spacing resulting in 30% open area. Each grid is 0.1" from each other with the exception of the front floating grid which is 0.2" from the first electron repeller. The ion repeller grid was swept from 0 V to 300 V for each trace. The current collected by the probe was then passed through a current amplifier and recorded by an oscilloscope. The anode and RPA were both referenced to cathode for data acquisition. In calculating the acceleration efficiency the repelling voltages were adjusted to be relative to ground potential (excerpt from reference³).

IV. Results

Figure 1 is the thrust efficiency as derived from thrust stand measurements. Efficiency reached a maximum of 11% at 100 V, 26% at 150 V, and 45% at 200 V. Magnet current settings for maximum thrust efficiency were 0.5 A, 1.5 A, and 1.75 A respectively. These magnet current

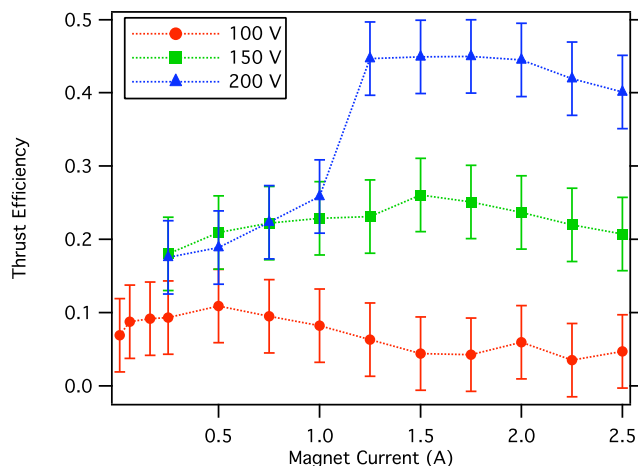


Figure 1. Thrust efficiency as calculated from thrust stand data.

values are comparable (to within .25 A) with the values used in the preceding study.³

A. Current Efficiency

Figure 2 depicts the current to the anode as a function of the magnet current. The current efficiency is the ratio of discharge current to mass-flow current multiplied by the ionization charge quantity $f_i Q$. For higher discharge voltages, $f_i Q$ is nearly unity meaning complete single ionization of the propellant.⁷ In low voltage operation propellant ionization drops and f_i decreases. The calculation of current efficiency measurements in figure 3 do not include the ionization charge quantity. This is equivalent to assuming that the propellant is entirely singly-ionized. This will give rise to an overestimation of the current efficiency in the event of poor ionization which becomes apparent in the 100 V trial when the 'efficiency' climbs above unity. The efficiency values for magnet currents 2.0 and 2.5 A in the 100 V trial reach above the axis limit to 1.8 and 2.4 respectively and show that the majority of the propellant is no longer ionized, $f_i Q \ll 1$. In 200 and 150 V cases

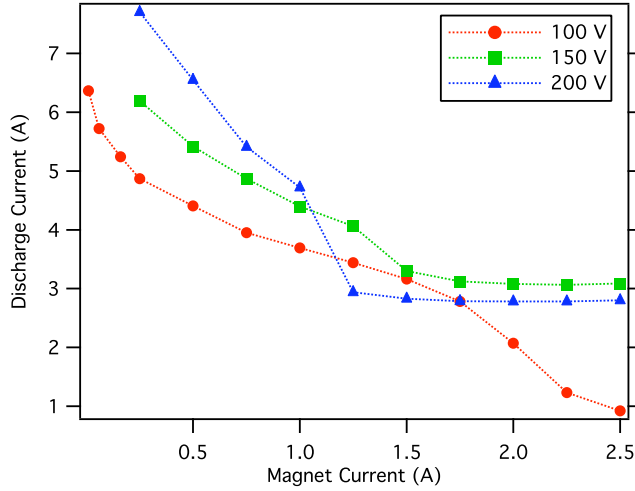


Figure 2. Discharge current as a function of magnet current for three discharge voltages at 3 mg/s.

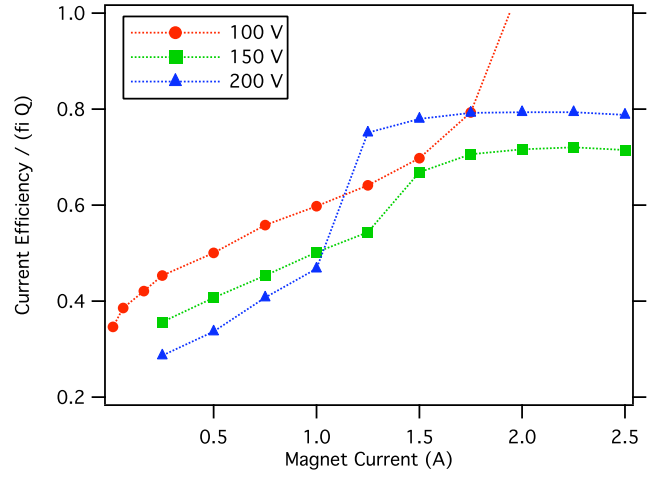


Figure 3. Current efficiency over the ionization charge quantity as a function of magnet current for three discharge voltages.

the current and efficiency plateaus above magnet currents of 1.5 A, likely indicating a minimum mobility current and a maximum ionization of the propellant, $f_i Q \approx 1$.

B. Acceleration Efficiency

A potential field is created between the anode and cathode as set by the discharge voltage. Exhausted ions are accelerated through a portion of this field. The acceleration efficiency is a measure of how much of this potential the average ion falls through. This can be calculated by recording the ion energies in the exhausted plume through the use of an RPA probe. The distribution functions produced by the RPA are used in equation 8 to obtain acceleration efficiencies. An RPA records ions as energy-per-charge which is equivalent to the effective acceleration potential since

$$\langle V_{eff} \rangle = \frac{\frac{1}{2}m \langle \mathbf{V}^2 \rangle}{f_i Q e} \quad (10)$$

So, while the RPA is insensitive to the ion charge number, the data is suitable to calculate acceleration efficiency. The differential RPA traces for a selection of current values for the 100 V case are displayed in figure 4.

Exhausted ions in the plume continually "push" on the thruster until they cease to accelerate or recombine with an electron and are neutralized. In ground testing, an ion continues to accelerate until it reaches terminal potential, the tank wall (ground). Therefore the distribution functions are adjusted relative to ground potential. In the case of ion-neutral charge exchange collisions, which are prevalent in ground testing, the newly born 'slow' ions will accelerate through the remainder of the potential field, providing thrust until they reach the wall. Since taking RPA traces at the tank wall is impractical, the amount of energy the ion gains between the RPA position and the tank wall can be recorded with an emissive probe to determine V_{plasma} with respect to ground and adding this amount of energy to the RPA trace, since this would encompass the total energy imparted to the ion during its interaction with the thruster.

Figure 5 displays the acceleration efficiency as a function of magnet current. As noted in reference,³ the efficiency increases with decreasing magnet current. In the 100 V trial the acceleration efficiency is above 70% even after the magnet power supply is turned off.

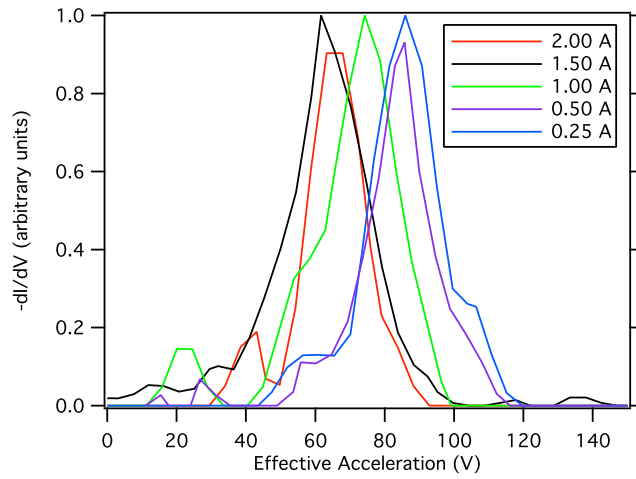


Figure 4. Differential RPA traces for a selection of magnet current values at 100 V discharge voltage and 3 mg/s. The traces are peak normalized.

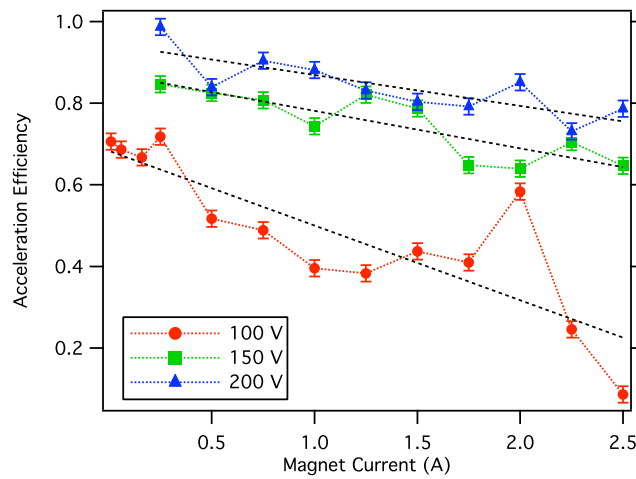


Figure 5. Acceleration efficiency as a function of magnet current for three discharge voltages.

V. Discussion

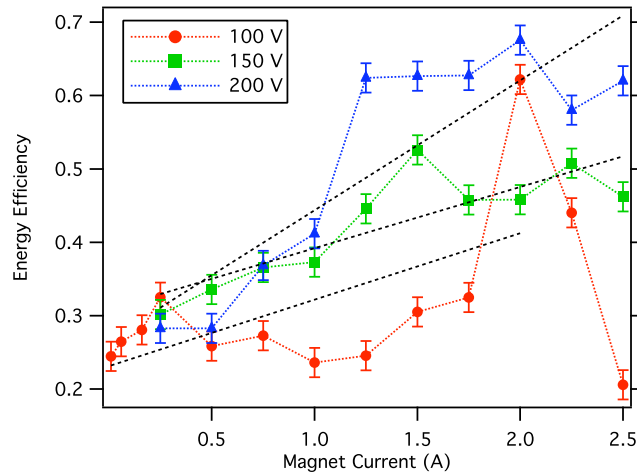


Figure 6. Energy efficiency as calculated from the acceleration efficiency and current efficiency. In the 100 V trial the values for 2.0 and 2.5 A were not included in the calculation of the linear fit.

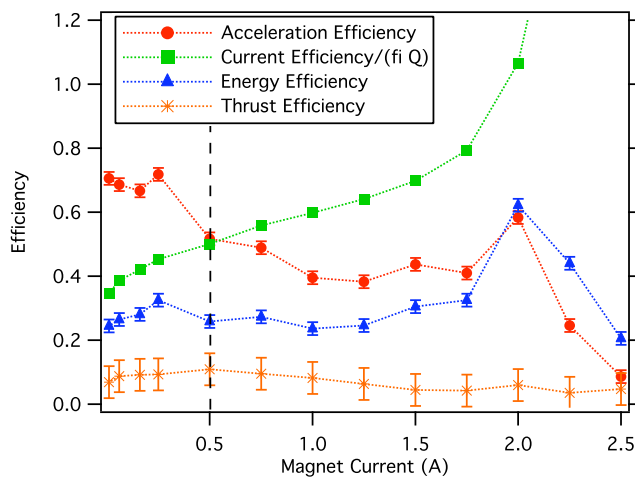


Figure 7. Acceleration, current, thrust and energy efficiencies for 100 V discharge potential. Dashed lines represent maximum thrust efficiency

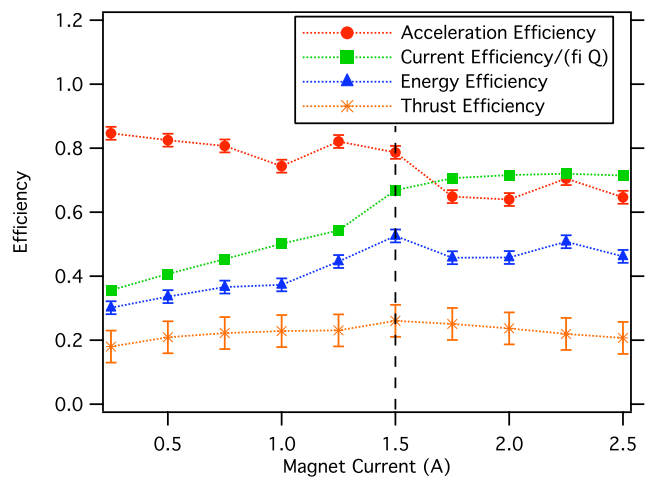


Figure 8. Acceleration, current, thrust and energy efficiencies for 150 V discharge potential. Dashed lines represent maximum thrust efficiency

All four of the efficiencies are displayed in figures 7-9 for a given discharge voltage. The dashed lines highlight the operating condition corresponding to maximum thrust efficiency. Interestingly, the diverging current efficiency and acceleration efficiency are equal to one another at maximum thrust efficiency for all three discharge voltages to within one current step size. Furthermore, the acceleration immediately increases to the left (less magnet current) of the maximum thrust efficiency.

Current efficiency reaches a maximum at a higher level of magnet current than at maximum thrust efficiency in all three trials. There is considerable research regarding relationship between current efficiency and magnetic field curvature and strength.⁸ The magnetic field controls the Hall current and subsequently much of the electron mobility characteristics contributing to large discharge current/low current efficiency. The acceleration efficiency's dependence on the magnet

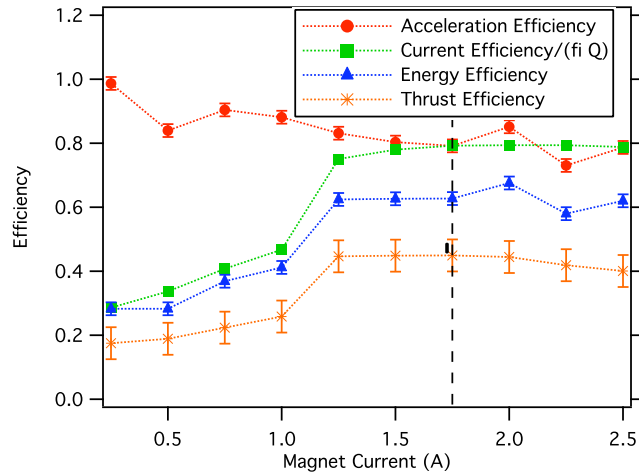


Figure 9. Acceleration, current, thrust and energy efficiencies for 200 V discharge potential. Dashed lines represent maximum thrust efficiency

field strength, however, is largely unknown.

As mentioned before, the potential field is subject to the cathode-to-ground potential. A decrease in the separation in the cathode-to-ground potential is directly an increase to the potential field available to the ion according to:

$$\Phi_{max} = V_d + \Phi_{CTG} \quad (11)$$

where Φ_{CTG} is negative.

In figure 10 the cathode-to-ground potential is shown to decrease by over 15 V in the 200 V trial and by 8 and 10 V for 150 and 100 V discharge respectively. This equates to an increase in acceleration of efficiency of 7.5%, 5.3%, and 10% for 200, 150, 100 V discharge voltages accounting for more than half of the increase of acceleration efficiency observed in RPA data in each trial.

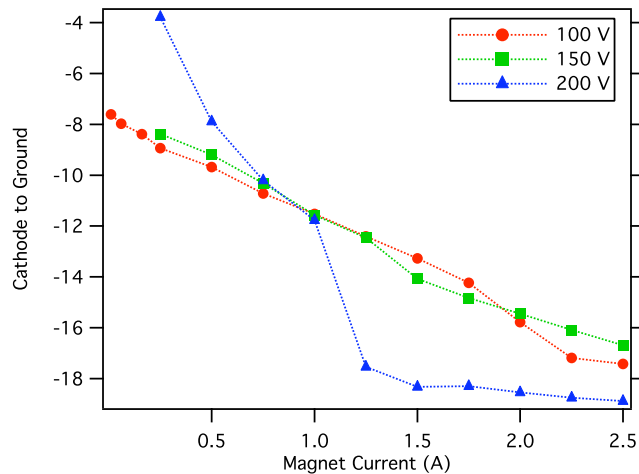


Figure 10. cathode-to-ground potential as a function of magnet current

The cathode-to-ground voltage accounts for 37%, 27%, and 33% of the increase in acceleration efficiency for 200, 150, and 100 V respectively. The source of the remaining increase in acceleration efficiency remains unaccounted for.

VI. Conclusions

Probe studies and thrust stand measurements were performed on Aerojet's BPT-2000 at discharge voltage from 200 V - 100 V for 3 mg/s flow of xenon. Thrust efficiency peaked at 0.5 A, 1.5 A, and 1.75 A for 100, 150 and 200 V respectively. Acceleration efficiency, as determined from RPA data, increased in value by 30, 20, and 20% for 100, 150 and 200 V over magnet current values beginning at 2.5 A and decrease incrementally to 0.25 A. The cathode-to-ground potential accounted for 33%, 27%, and 37% of the increase in acceleration efficiency. A first step in improving Hall thruster operation at low discharge voltages can be approached by attempting to reduce the cathode-to-ground potential for higher magnet current levels.

VII. Acknowledgments

The authors would like to thank Dr. Bill Larson of the Air Force Research Laboratories for his discussions on acceleration efficiency and ionization charge quantity, and Aerojet for the use of their BPT-2000 Hall thruster. This research was funded by the National Science Foundation and the Air Force Office of Scientific Research.

References

- ¹Britt, E. J. N. and McVey, J. B., "ELECTRIC PROPULSION ACTIVITIES IN U.S. INDUSTRIES," *38th AIAA/ASME/SAE/ASEE Joint Propulsion Conference & Exhibit*, Vol. AIAA 2002-3559, Indianapolis, Indiana, July 7-10 2002.
- ²Manzella, D. and Jacobson, D., "Investigation of Low-Voltage/High-Thrust Hall Thruster Operation," *39th AIAA/ASME/SAE/ASEE Joint Propulsion Conference & Exhibit*, Vol. AIAA-2003-5004, Huntsville, Alabama, July 20-23 2003.
- ³Ross, J. L., Sommerville, J. D., and King, L. B., "Efficiency Mechanisms of a Low Discharge Voltage Hall Thruster," *Journal of Propulsion and Power*, Vol. submitted July 2007, 2007.
- ⁴C. William Larson, D. L. B. and William A. Hargus, J., "Thrust Efficiency, Energy Efficiency, and the Role of the VDF in Hall Thruster Performance Analysis," *43rd AIAA/ASME/SAE/ASEE Joint Propulsion Conference and Exhibit*, Vol. AIAA 2007-5270, Cincinnati, OH, July 8-11 2007.
- ⁵D. King, D. Tilley, R. A. K. N. R. S. C. R. V. H. B. P. J. M., "Development of the BPT family of U.S.-designed Hall current thrusters for commercial LEO and GEO applications," *34th AIAA/ASME/SAE/ASEE Joint Propulsion Conference and Exhibit*, Cleveland, Ohio, July 13-15 1998.
- ⁶Haag, T. W., "Design of a thrust stand for high power electric propulsion devices," *25th AIAA/ASME/SAE/ASEE Joint Propulsion Conference & Exhibit*, Vol. AIAA-1989-2829, Monterey, CA, July 10-13 1989.
- ⁷Hofer, R. R. and Gallimore, A. D., "Efficiency Analysis of a High-Specific Impulse Hall Thruster," *40th AIAA/ASME/SAE/ASEE Joint Propulsion Conference & Exhibit*, Vol. AIAA-2004-3602, Ft. Lauderdale, Florida, July 11-14 2004.
- ⁸Fossum, E. C. and King, L. B., "Design and Construction of an Electron Trap for Studying Cross-Field Mobility in Hall Thrusters," *43rd AIAA/ASME/SAE/ASEE Joint Propulsion Conference and Exhibit*, Vol. AIAA-2007-5207, Cincinnati, OH, July 8-11 2007.